Molecular sublayers beneath the air-sea interface relative to momentum, heat and gas transports

Wu-ting Tsai,[1,2] Shi-Ming Chen,[2] Mei-Ying Lin,[2] and Li-Ping Hung[2]

Received 14 July 2003; accepted 27 August 2003; published 27 September 2003.

[1] Numerical simulations of the wind-driven aqueous turbulent flow and the underlying heat and dissolved gas transports are conducted with sufficiently fine grid resolution to resolve the molecular sublayers immediately beneath the air-water interface. The simulated mean distributions of velocity, temperature and gas concentration all exhibit exponential profiles across the sublayers in accordance with the theoretical postulation of *Liu and Businger* [1975] which they derived on the basis of the conceptual surface renewal model. The numerical results identify two major coherent renewal processes within the flow: intermittent upwellings induced by uprising horseshoe-like eddies in the well-mixed region, and elongated, high-speed, cool streaks within the sublayer reflecting the cool-skin thermal structure. *INDEX TERMS:* 0312 Atmospheric Composition and Structure: Air/sea constituent fluxes (3339, 4504); 4504 Oceanography: Physical: Air/sea interactions (0312); 4568 Oceanography: Physical: Turbulence, diffusion, and mixing processes; 4524 Oceanography: Physical: Fine structure and microstructure. **Citation:** Tsai, W.-T., S.-M. Chen, M.-Y. Lin, and L.-P. Hung, Molecular sublayers beneath the air-sea interface relative to momentum, heat and gas transports, *Geophys. Res. Lett.*, *30*(18), 1968, doi:10.1029/2003GL018164, 2003.

1. Introduction

[2] The air-sea interface drastically damps the vertical turbulent motions within a layer of a few millimeters immediately next to the interface. Accordingly, the cross-boundary transports of both momentum and scalar are dominated via molecular diffusion. For momentum transfer, the shear stress is transmitted across the viscous sublayer by molecular viscosity. This viscous sublayer was previously found to be thinner than the analogous sublayer in close proximity to a solid no-slip wall [*Csanady*, 1984; *Wu*, 1984]. For heat exchange with net upward heat flux, a similar conductive sublayer forms, which results in an ocean skin cooler than that of the underlying water to the order of 0.1–0.5 K [*Katsaros*, 1980]. Recent renewed interest in this subject has been provoked by the need to improve the validation of satellite-derived sea surface temperature using *in situ* bulk temperature [*Donlon et al.*, 2002]. Accurately estimating bulk air-sea flux using *in situ* temperature measurements also requires correction for such a cool-skin effect [*Fairall et al.*, 1996a].

[3] Because of the difficulties inherent in the measurements, both field and laboratory experiments which attempt to reveal the flow structure within the few millimeters beneath the interface have been rare. Examples of the few attempts include velocity measurements by *McLeish and Putland* [1975] and *Wu* [1984]; as well as temperature measurements by *Khundzhua and Andreyev* [1974] and *Mammen and von Bosse* [1990]. Much of the previous description of this sublayer was drawn from our understanding of the flow next to a no-slip solid wall. *Brutsaert* [1975] and *Liu and Businger* [1975] were the very first to derive physics-based approximations of mean passive scalar profiles by matching the molecular diffusion process to the turbulent renewal model of *Danckwerts* [1951]. The renewal model postulates that the sublayer undergoes cyclic growth and disruption by the turbulent eddies randomly emerge from the well-mixed turbulent layer. The exchange is enhanced when the eddies impinge the interface, temporarily destructing the sublayers. Motivated by the near-surface temperature measurements of *Khundzhua and Andreyev* [1974], *Liu and Businger* [1975] derived an exponential profile for the mean temperature distribution within the thermal sublayer by assuming a Gaussian renewal process. Adopting such a profile function and extending it to velocity and humidity, *Liu et al.* [1979] further developed a bulk parameterization for air-sea fluxes. Recent improvements of this bulk method [e.g., *Fairall et al.*, 1996b] are essentially extension of the *Liu et al.* [1979] model. Despite the wide acceptance of the surface renewal model in air-sea flux parameterizations, the renewal events have mostly been inferred from the images at the water surface. For instance, *Jessup et al.* [1997], *Zappa et al.* [1998] and *Haussecker et al.* [2002], among many others, used infrared imagery to identify the events and to further quantify the processes, such as wave breaking and heat transport, which form the thermal signatures. The underlying "renewal eddies" in the process, nevertheless, remain to be conceptual and have never been actually visualized.

[4] The formation mechanisms of these surface renewal events are determined by various environmental factors, such as shear turbulence, wave motions and breaking, which govern the forced convections beneath the interface. In this study, we focus on the renewal processes attributed to a turbulent shear layer induced by wind stress acting at the interface. The primary objective, therefore, is two-fold: to validate the mean profile derived by *Liu and Businger* [1975] that has been widely employed in bulk parameterization of air-sea fluxes; and to characterize the flow

[1]Institute of Hydrological Sciences, National Central University, Taoyuan, Taiwan.
[2]Department of Civil Engineering, National Chiao Tung University, Hsinchu, Taiwan.

0094-8276/03/2003GL018164

structures and surface signatures associated with the underlying renewal events within the sublayer.

2. Numerical Model

[5] To understand the underlying processes of the renewal model, a canonical problem of the wind-driven turbulent shear flow as well as the distributions of the temperature and concentration associated with heat and gas transports are simulated numerically. The numerical model is an extension of *Tsai* [2001, 2002] that has been tested and validated in a previous study [*Tsai*, 1998]. With the emphasis on resolving the molecular sublayer in simulating the turbulent boundary layer, no turbulence parameterizations are used to model the subgrid momentum and passive scalar transports. An adaptive grid system is employed such that the resolution of discretization increases when approaching the interface with approximately 30 grids points located within the sublayer. As a reference for validating the model results, the wind-driven shear currents in the controlled laboratory experiments of *Melville et al.* [1998] and *Veron and Melville* [2001] are simulated. Three flow conditions corresponding to the subsequent developments of the shear turbulence at the final wind speeds of U_a = 3, 4 and 5 m s^{-1}, are considered in the present simulations.

3. Mean Profiles

[6] Adopting the formulation of *Liu and Businger* [1975] and expressing the vertical variation in wall coordinate $z^+ = zu_*\nu$, the mean velocity profile across the viscous sublayer driven by a constant shear stress τ_0 at the interface is [*Kraus and Businger*, 1994]:

$$\frac{u_0 - \overline{u}(z)}{u_*} = \xi_u \left[1 - \exp\left(-\frac{z^+}{\xi_u}\right)\right], \tag{1}$$

where $\overline{u}$ represents the temporal or horizontal-spatial average of the streamwise velocity; $u_0 = \overline{u}(0)$ is the mean surface velocity; $u_* = (\tau_0/\rho)^{1/2}$ is the friction velocity; ρ and ν are the density and kinematic viscosity, respectively. The non-dimensional sublayer parameter $\xi_u = \delta_u u_*/\nu$ determines the thickness of viscous sublayer $\delta_u = (\nu t_u)^{1/2}$, where t_u is the characteristic residence duration of the renewal fluid elements. Beneath the sublayer but not too far from the interface, the well-mixed flow is found to be characterized by the logarithmic profile [*Churchill and Csanady*, 1983; *Wu*, 1975]:

$$\frac{u_0 - \overline{u}(z)}{u_*} = \frac{1}{\kappa}\ln z^+ + \psi^+ = \frac{1}{\kappa}\ln\frac{z}{z_0}, \tag{2}$$

where κ is the von Karman constant; and the integration constant ψ^+ is related to surface roughness z_0 by $\kappa\psi^+ = -\ln(u_* z_0/\nu)$. The two-layer model of *Liu et al.* [1979] requires matching of the exponential and logarithmic profiles, (1) and (2). Equating the right-hand sides and their first derivatives of (1) and (2) at a matching coordinate $z^+ = \zeta_u^+$ yields two nonlinear equations for the sublayer parameter ξ_u and the matching depth ζ_u^+.

[7] The profiles of the simulated mean streamwise velocity, $(u_0 - \overline{u}(z))/u_*$, are shown in Figure 1 for the three reference wind speeds u_a = 5.0, 4.0 and 3.0 m s^{-1}. The numerical results are compared with the parameterized exponential and logarithmic profiles, (1) and (2). Also plotted in the figure are the experimental measurements of *Wu* [1984] for the wind speeds of 4.8, 4.0 and 3.0 m s^{-1}. The experimental data scatter but the distributions of the mean values remain close to the present simulated profiles. The numerical simulations, the experimental measurements and the parameterized profiles are comparative throughout the whole sublayer range extending to the buffer zone. In reaching the logarithmic profile, the non-dimensional constants κ and ψ^+ are determined by a least-squares fit to the averaged velocities for the depths z^+ = 20 to 100. The computed values of κ are between 0.35 and 0.40, close to the universal von Karman constant, 0.4. The typical values of computed ψ^+ are around 1.0 for the simulations of u_a = 5 ms^{-1}, 1.5 for u_a = 4 ms^{-1} and 1.9 for u_a = 3 ms^{-1}. These are, in fact, much smaller than 5.0 for a no-slip smooth wall. The decrease in the integration constant ψ^+ indicates an increase in equivalent surface roughness, and infers the enhancement of near-surface ''horizontal'' turbu-

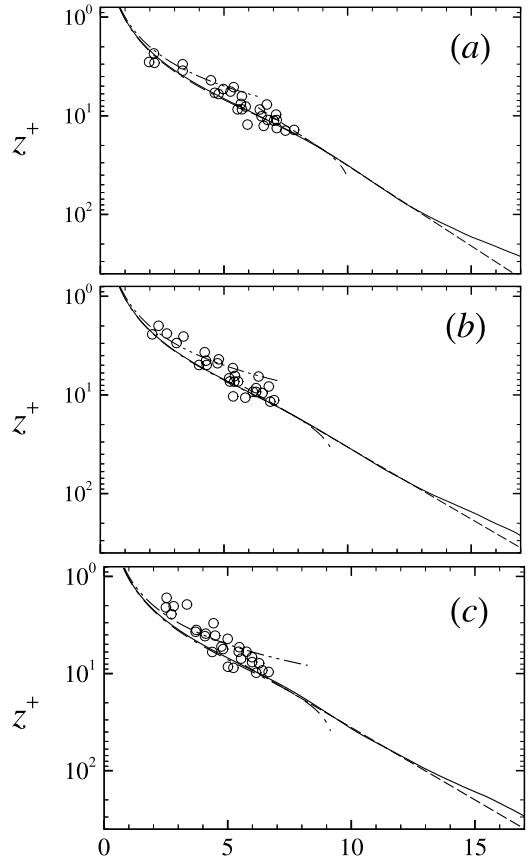

Figure 1. Distributions of the mean streamwise velocities for various wind speeds: u_a = 5 m s^{-1} (a), 4 ms^{-1} (b) and 3 ms^{-1} (c). The computed results are represented by solid curves. The dash-dotted curves are the exponential profiles within the viscous sublayer (1) developed based on the surface renewal model of *Liu and Businger* [1975], and the dash-dot-dotted curves are the traditional linear profiles. The dashed curves are the fitted logarithmic distributions (2) from the numerical profiles. The circular symbols are laboratory measurements of *Wu* [1984].

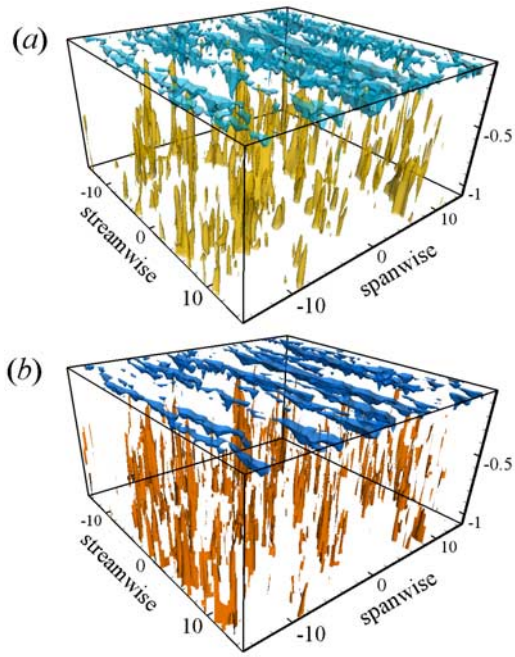

Figure 2. Representative isosurfaces of instantaneous temperature (a) and streamwise and vertical velocities (b). The direction of flow is out of the page. The temperature values of the isothermal surfaces are 60% and 90% of the mean bulk temperature, and the streamwise and vertical velocities are 114% and 7% of the mean surface velocity, representative of the cool, high-speed streaks within the sublayer and the warm upwellings from the well-mixed region, respectively.

lence intensity. This finding is similar to the field observations of *Churchill and Csanady* [1983] and the laboratory measurements by *Wu* [1975, 1984]. The computed non-dimensional sublayer parameters ξ_u are 9.8, 10.5 and 11.2 corresponding to the dimensional thicknesses of the viscous sublayers δ_u = 1.4, 1.6 and 1.9 mm, respectively, for the three reference wind speeds of u_a = 5, 4 and 3 ms^{-1}. Although these values of ξ_u are smaller than that immediately below a smooth no-slip wall (ξ_u = 16) [*Liu et al.*, 1979], the near-surface flow characteristics are qualitatively similar to those observed in the experiments [*Csanady*, 1984; *Wu*, 1984]. The thickness of the viscous sublayer increases with decreasing wind speed implying the growth of resistance against the vertical momentum transport.

[8] For heat transfer across a thermal sublayer, the given heat flux across the interface Q gives rise to a Neumann condition for the temperature θ at the interface as $\partial\theta(0, t)/\partial z = -Q/(\rho c_p \nu_\theta)$, where c_p and ν_θ are the specific heat and heat diffusivity of water, respectively. As for the air-water flux of sparingly soluble gases, the resistance is dominated by the aqueous flow and the atmosphere can be regarded as an infinite reservoir with the gas concentration $c = c_0$ given at the interface as a Dirichlet condition. Despite the different interfacial conditions, similar exponential profiles can be obtained for temperature and concentration distributions within the sublayers as (1). Similar to the velocity distribution, the computed mean temperature and gas concentration distributions for the corresponding velocity profiles of Figure 1 are also well represented by the exponential-logarithmic matched functions.

4. Flow and Thermal Structures

[9] The spatial distributions of representative temperature and velocity isosurfaces near the interface are shown in Figure 2 to depict the thermal and flow structures within the sublayers as well as the renewal processes arising from the turbulence region. Within the thermal sublayer, elongated isothermal surfaces with temperatures lower than the mean temperature are observed (Figure 2(a)). The region of cold waters correlates well with that of high-speed jets inside the viscous sublayer (Figure 2(b)). These elongated structures are characterized by wind-aligned streaks at the interface. Away from the cool thermal sublayer, warm isothermal surfaces stick vertically out of the well-mixed region. Examining the isosurfaces of upward velocity, it becomes clear that these "warm tongues" are attributed to flows welling up from the submerged turbulent layer. These upwellings are induced by the uprising Ω-shaped horseshoe-like vortices evolving from the mean shear driven by the interfacial stress [*Tsai*, 1998]. As these Ω-shaped eddies move upwards and impinge the interface, they induce upwelling flows, thereby enhancing the renewal of water in contact with the interface. Since the submerged fluids convect with lower mean streamwise velocities than those of the upper layer, the local streamwise velocities within these upwellings are also lower than those in the surrounding flows. In contrast to the elongated cold steaks within the laminar sublayer which are organized with somewhat equal spacing, the warm tongues well up intermittently from the turbulence region without any coherency. At the cool skin, these upwellings form slowly-moving, warm, localized spots. Such mixed thermal

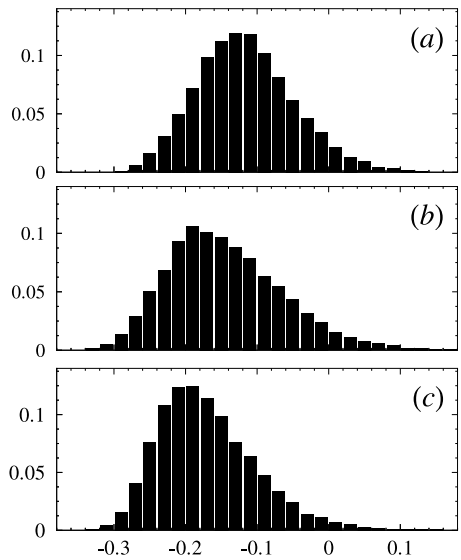

Figure 3. Histograms of the deviation of the skin temperature θ_0 from the sub-skin temperature $\theta_{subskin}$, $\Delta\tilde{\theta} = (\theta_0 - \theta_{subskin})/\theta_{subskin}$, for the three reference wind speeds: u_a = 5 ms^{-1} (a), 4 ms^{-1} (b) and 3 ms^{-1} (c). The histograms are normalized by the total numbers of data samples taken over time intervals.

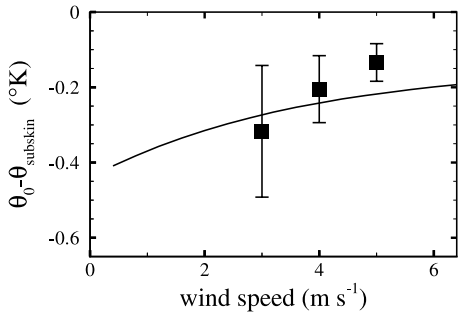

Figure 4. Relationship between the deviations of skin temperature from the sub-skin temperature $\Delta\theta = \theta_0 - \theta_{subskin}$ and the wind speed. The circular symbols denote the averaged numerical results from various time instants of the simulations, while the error bars represent variations. The solid curve is the fitted function of *Donlon et al.* [2002]: $\Delta\theta = -0.14 - 0.30 \exp(-U/3.7)$.

signatures, with elongated cool streaks and warm spots coexisting at the water surface, have recently been observed in both field and laboratory experiments [*Haussecker et al.*, 2002; *Melville et al.*, 1998; *Veron and Melville*, 2001].

[10] To further elucidate the attribution of the three-dimensional thermal structure to the well-known cool-skin feature, probability distributions of the deviation of the skin temperature θ_0 from the sub-skin temperature $\theta_{subskin}$, $\Delta\tilde{\theta} = (\theta_0 - \theta_{subskin})/\theta_{subskin}$, are shown in Figure 3 for the three reference wind speeds. The sub-skin temperature is defined as the temperature at the edge of the thermal sublayer, $\theta_z = \delta_\theta$. The histograms exhibit negative skewness with variations ranging $-0.3 < \Delta\tilde{\theta} < 0.1$. Quantitatively similar to the field observations [e.g., *Donlon et al.*, 2002], the skewness of the distribution is prevalent for lower wind speeds. By least-squares fitting of various measurement data sets, *Donlon et al.* [2002] found the dependence of the skin temperature deviation $\Delta\theta$ on the wind speed U can be adequately represented by $\Delta\theta = -0.14 - 0.30 \exp(-U/3.7)$. For a prescribed heat flux $Q = 100$ Wm^{-2}, the simulated dimensional temperature deviations are plotted in Figure 4 to compare with the fitted function. The simulated mean skin temperature deviations decrease with increasing wind speed as in field observations. The modeled results, which include only the mechanism of shear-produced turbulence in the formation of the cool-skin sublayer, have a higher decreasing rate than the regression relationship from field measurements. However, the close comparison between the predicted and measured results confirms the observation of *Donlon et al.* [2002] that wind-induced shear-driven turbulent transport is the dominant process governing the air-sea heat exchange. We note that the net heat flux Q is still a free parameter in determining the dimensional temperature deviations in Figure 4 from the results of model simulation. With additional variables involved in the open oceans, it seems infeasible to parameterize the skin-temperature deviations solely using the wind speed as a variable.

5. Concluding Remarks

[11] It is acknowledged that other environmental factors, such as spray and air entrainment caused by wave breaking at high wind speeds, also contribute to the air-sea transport processes. The low wind speed and non-breaking conditions considered in this study therefore represent only part of the global ocean surfaces. Yet these are exactly the conditions under which accurate satellite-derived sea-surface temperatures can be obtained. Furthermore, the surface renewal model discussed in the present study is valid for low to moderate wind speeds where the interface is more or less intact. Despite the limitation, surface renewal theory is still among the most widely used model in the bulk formulation of air-sea transfer fluxes. Through high-resolution numerical simulations, in this study we reveal the detailed underlying physics in the renewal processes and confirm the first-order statistics derived based on the theory. In addition, the molecular sublayer is found to exhibit not only random temporal and spatial variabilities induced by the renewal eddies, but also organized velocity and thermal structures. Such organized structures within the molecular sublayer are ingeniously correlated to the formation of a cooler ocean skin.

[12] **Acknowledgments.** This work was supported by grants from the National Science Council of Taiwan (NSC 89-2611-M-009-004 and 90-2611-M-009-001).

References

Brutsaert, W., A theory for local evaporation (or heat transfer) from rough and smooth surfaces at ground level, *Water Resour. Res.*, *11*, 543–550, 1975.

Churchill, J. H., and G. T. Csanady, Near-surface measurements of quasi-Lagrangian velocities in open water, *J. Phys. Oceanogr.*, *13*, 1669–1680, 1983.

Csanady, G. T., The free surface turbulent shear layer, *J. Phys. Oceanogr.*, *14*, 402–411, 1984.

Danckwerts, P. V., Significance of liquid-film coefficients in gas absorption, *Ind. Eng. Chem.*, *43*, 1460–1467, 1951.

Donlon, C. J., P. J. Minnett, C. Gentemann, T. J. Nightingale, I. J. Barton, B. Ward, and M. J. Murray, Toward improved validation of satellite sea surface skin temperature measurements for climate research, *J. Clim.*, *15*, 353–369, 2002.

Fairall, C. W., E. F. Bradley, J. S. Godfrey, G. A. Wick, J. B. Edson, and G. S. Young, Cool-skin and warm-layer effects on sea surface temperature, *J. Geophys. Res.*, *101*, 1295–1308, 1996a.

Fairall, C. W., E. F. Bradley, D. P. Rogers, J. B. Edson, and G. S. Young, Bulk parameterization of air-sea fluxes for Tropical Ocean Global Atmosphere Coupled Ocean Atmosphere Response Experiment, *J. Geophys. Res.*, *101*, 3747–3764, 1996b.

Haussecker, H. W., U. Schimpf, C. S. Garbe, and B. Jähne, Physics from IR image sequences: Quantitative analysis of transport modes and parameters of air-sea gas transfer, in *Gas Transfer at Water Surfaces*, AGU Monograph Ser., *127*, edited by M. A. Donelan, W. M. Drennan, E. S. Saltzman, and R. Wanninkhof, pp. 103–108, AGU, Washington D. C., 2002.

Jessup, A. T., C. J. Zappa, M. R. Loewen, and V. Hesany, Infrared remote sensing of breaking waves, *Nature*, *385*, 52–55, 1997.

Katsaros, K. B., The aqueous thermal boundary layer, *Boundary-Layer Meteorol.*, *18*, 107–127, 1980.

Khundzhua, G. G., and Ye. G. Andreyev, An experimental study of heat exchange between the ocean and the atmosphere in small-scale interaction, *Izv. Atmos. Oceanic Phys.*, *10*, 1110–1113, 1974.

Kraus, E. B., and J. A. Businger, *Atmosphere-Ocean Interaction*, Oxford Univ. Press, New York, 1994.

Liu, W. T., and J. A. Businger, Temperature profile in the molecular sublayer near the interface of a fluid in turbulent motion, *Geophys. Res. Lett.*, *2*, 403–404, 1975.

Liu, W. T., K. B. Katsaros, and J. A. Businger, Bulk parameterization of air-sea exchanges of heat and water vapor including the molecular constraints at the interface, *J. Atmos. Sci.*, *36*, 1722–1735, 1979.

Mammem, T. C., and N. von Bosse, STEP - A temperature profiler for measuring the oceanic thermal boundary layer at ocean-air interface, *J. Atmos. Ocean Tech.*, *7*, 312–322, 1990.

McLeish, W., and G. E. Putland, Measurements of wind-driven flow profiles in the top millimeter of water, *J. Phys. Oceanogr.*, *5*, 516–518, 1975.

Melville, K., R. Shear, and F. Veron, Laboratory measurements of the generation and evolution of Langmuir circulations, *J. Fluid Mech.*, *364*, 31–58, 1998.

Tsai, W.-T., A numerical study of the evolution and structure of a turbulent shear layer under a free surface, *J. Fluid Mech.*, *354*, 239–276, 1998.

Tsai, W.-T., On the formation of streaks on wind-driven water surfaces, *Geophys. Res. Lett.*, *28*, 3959–3962, 2001.

Tsai, W.-T., Numerical simulation of hydrodynamic processes beneath a wind-driven water surface, in *Gas Transfer at Water Surfaces*, AGU Monograph Ser. *127*, edited by M. A. Donelan, W. M. Drennan, E. S. Saltzman, and R. Wanninkhof, pp. 71–75, AGU, Washington D. C., 2002.

Veron, F., and W. K. Melville, Experiments on the stability and transition of wind-driven water surfaces, *J. Fluid Mech.*, *446*, 25–65, 2001.

Wu, J., Wind-induced drift currents, *J. Fluid Mech.*, *68*, 49–70, 1975.

Wu, J., Viscous sublayer below a wind-disturbed water surface, *J. Phys. Oceanogr.*, *14*, 138–144, 1984.

Zappa, C. J., A. T. Jessup, and H. Yeh, Skin layer recovery of free-surface wakes: Relationship to surface renewal and dependence on heat flux and background turbulence, *J. Geophys. Res.*, *103*, 21,711–21,722, 1998.

W.-T. Tsai, Institute of Hydrological Sciences, National Central University, Jungli City, Taoyuan, 320, Taiwan. (wttsai@cc.ncu.edu.tw)

S.-M. Chen, M.-Y. Lin, and L.-P. Hung, Department of Civil Engineering, National Chiao Tung University, Hsinchu 300, Taiwan.